CORROSION SCIENCE AND TECHNOLOGY, Vol.18, No.6(2019), pp.243~252
[Research Paper]
pISSN: 1598-6462 / eISSN: 2288-65245
DOI: https://doi.org/10.14773/cst.2019.18.6.243

# Corrosion Behavior and Inhibition Studies of AZ31B Magnesium Alloy With and Without $Cl^-$ in the Alkaline Electrolytes in Addition with Various Inhibitor Additives

**Yoonji Shin and Kyehyun Cho†**

*School of Materials Science and Engineering, Yeungnam University, Daehak-Ro 280, Gyeongsan, Gyeongbuk 712-749, South Korea*

(Received October 24, 2019; Revised November 29, 2019; Accepted November 29, 2019)

The pitting corrosion and inhibition studies of AZ31B magnesium alloy were investigated in the alkaline solution (pH12) with chloride and inhibitors. The corrosion behavior of passive film with/without $Cl^-$ in the alkaline electrolyte were conducted by polarization curve and immersion tests in the presence of various additives (inhibitors) to clarify the inhibition efficiency of pitting corrosion at higher potential region. Critical concentration of pitting corrosion for Mg alloy was evaluated with 0.005 M NaCl in 0.01 M NaOH on the anodic polarization behavior. Critical pitting of AZ31B Mg alloy in 0.01 M NaOH is a function of chlorides; $E_{pit}$ = - 1.36 – 0.2 log [$Cl^-$]. When the Sodium Benzoate (SB) was only used as an inhibitor, a few metastable pits developed on the Mg surface by an immersion test despite no pitting corrosion on the polarization curve meaning that adsorption of SB on the surface is insufficient protection from pitting corrosion in the presence of chloride. The role of SB and Sodium Dodecylbenzenesulfonate (SDBS) inhibitors for the Mg alloy surface in the presence of chloride was suppressed from pitting corrosion to co-adsorb on the Mg alloy surface with strong formation of passive film preventing pitting corrosion.

***Keywords:*** *Magnesium alloy, Corrosion inhibitor*

## 1. Introduction

Recent developments in industry have caused concerns about environmental pollution and energy depletion for automotive applications. As a result, discussions on high-performance ultra-lightweight materials are actively being conducted in all industries for effective energy use. Among many lightweight materials, magnesium is the good candidate material due to the eighth most abundant element in the crust, with a specific gravity of 1.74 g/cm$^3$ which is very low density. Currently, surface treatment of AZ31B magnesium alloys also was hot issue for alkaline degreasing to prevent corrosion during surface pretreatment [1-5].

Therefore, magnesium alloys are attracting attention as high efficiency ultra-lightweight materials with advantages such as high noble strength and electromagnetic wave shielding, and they are being used in various fields such as automobile parts, aircraft parts, electronic parts and the like, and they are gradually increasing their application to the industrial parts.

†Corresponding author: kcho@ynu.ac.kr

However, if magnesium is inappropriately treated for protective coating on its surface, it will corrode very quickly in air or solution due to its high activity in aqueous electrolyte [2-5]. It is also long known that the stability of the passive layer of magnesium alloy can be ensured only in an alkaline electrolyte of pH 11 or higher than that of pH, which is a very narrow region among a wide range of pH values. Lunder *et al.* [6] was found that when the Al content reaches 8%, the Mg alloy exhibit good resistant in corrosion in NaCl solution. Lei Wang *et al.* [7] and other investigators [8,9] reported that corrosion behavior of AZ31B Mg alloy is good corrosion resistant compared with different Mg alloy in various concentration of NaCl with electrochemical test. However, the Mg alloys are still active in various service conditions, the reason for less corrosion resistant of Mg alloy resulted in primarily from two mechanisms; 1) formation of passive film on the surface is not perfect and protective: 2) galvanic or bimetallic corrosion could be caused by impurities and second phases [10].

Also, it was reported by Shengxi Li *et al.* [11] that the AZ31B Mg alloy exhibits the most stable and uniform passive film on the surface at pH12 alkaline electrolyte.

**Table 1 Chemical composition of AZ31B Mg alloy (wt%) for (a) sheet type and (b) bar type**

| | Mg | Al | Zn | Mn | Si | Fe | Cu | Ni | Be |
|---|---|---|---|---|---|---|---|---|---|
| (a) | Bal. | 4.094 | 0.910 | 0.387 | 0.027 | < 0.0012 | < 0.0005 | < 0.0010 | 0.0007 |
| (b) | Bal. | 2.638 | 0.916 | 0.406 | 0.026 | < 0.0012 | < 0.0005 | < 0.0015 | 0.0003 |

It also was observed that optimal passivation for the Mg alloy is very narrow pH at 12 due to the breakdown of the passive film in the vicinity on the intergranular boundaries. Later, the observation was made that AZ31B Mg alloy are highly susceptible to corrosion under salt-spray conditions and small amounts of NaCl concentration [12,13], so they are still limited in widening their applications to industry [14]. In order to find optimum condition for surface treatment in industry for Mg alloy, Jinsun Liao *et al.* [15] investigated the study of grain size effect for corrosion behavior. Also, Pardo *et al.* [16] and other groups [17,18] found that corrosion of magnesium alloys is very restricted to industrial applications. There were focused on the researches for stability of the passive film of AZ31B Mg alloy in alkaline solutions of pH12 [19].

The conventional methods of Mg alloy corrosion protection have been facing serious environmental problems in recent years [16-19]. The corrosion inhibition of Mg alloys was also observed upon surface treatment and/or incorporation of organic compounds into the passive layer. To minimize the disadvantage of Mg alloys in service life, inhibitor study of Mg alloy was inevitable. Therefore, a great number of researches have been made to subjects of inhibition studies [20-25] that corrosion inhibitors such as sodium benzoate (SB) in NaCl and 8-hydroxylquinoline and sodium dodecylbenzenesulphonate (SDBS) for magnesium alloy in NaCl solution were focused on protection for parts application during the surface treatment in artificial corrosive solution.

Therefore, in this study, we investigated the critical concentration of $Cl^-$ for pitting corrosion of Mg alloy in the alkaline solution (pH=12) for the surface treatment condition. In other words, the chloride concentration on pitting potential ($E_{pit}$) for Mg alloy in alkaline electrolyte is still working on relationship with a dependence of $E_{pit}$ on chlorine concentration. We will introduce whether or not to determine the new equation based on the experimental data from the pitting potential as an increase of chloride concentration which the passive state metal is expressed by the conventional form as a function of concentration of chloride

Also, the other main goals of this study were to investigate the stability of passive film AZ31B Mg alloy in the 0.01 M NaOH electrolyte with/without $Cl^-$ and inhibitors such as SB (Sodium Benzoate) and/or SDBS (Sodium Dodecylbenzenesulphonate) ; 1) the role of chloride ion in the alkaline electrolyte in the context of stability of passive film and pitting corrosion, 2) the effect of stability passive film for SB inhibition action in the presence of chlorides, 3) the stability of passive film and pitting corrosion for synergy SB and SDBS in the presence of chlorides.

## 2. Experimental

The composition of AZ31B Mg alloy supplied by Korean Mg Cooperation was listed as shown in Table 1. The samples for the electrochemical test were roll-milled in factory and was cut into samples by laboratory saws as the working electrode (WE). The specimens with a diameter of 10mm were polished to #800 ~ #2000 using SiC grit paper until mirror-like surface was obtained, and then successively the surface was ultrasonically washed with ethanol.

The various electrolyte solution, all containing the NaOH electrolyte (pH12); 1) 0.01 M NaOH, 2) 0.01 M NaOH + 0.005 M NaCl, 3) 0.01 M NaOH + 0.01 M NaCl, 4) 0.01 M NaOH + 0.02 M NaCl, 5) 0.01 M NaOH + 0.01 M NaCl + 0.5 M SB, and 6) 0.01 M NaOH + 0.01 M NaCl + 0.5 M SB + 0.005 M SDBS were prepared from reagent grade chemicals by double distilled water.

The experimental set-up and sample arrangement was shown in Fig. 1. The Electrochemical tests were carried out using a standard three electrode (RE, WE, CE) system to study the potentiodynamic polarization. The reference electrode (RE) consisted of a salt bridge tip and an SCE (Saturated Calomel Electrode) electrode embedded in a saturated KCl solution. The counter electrode (CE) was rod-shaped carbon.

The experiment procedures for the electrochemical polarization are as follows; the specimen was primarily immersed in the electrolyte before the polarization test, a voltage of - 2.0 V,SCE, (from now on all potential units are SCE scale) was applied for 900s before stabilizing of the sample. For the electrochemical test potentiodynamic method was introduced to evaluate polarization behavior by carrying out with scan potential ranging from

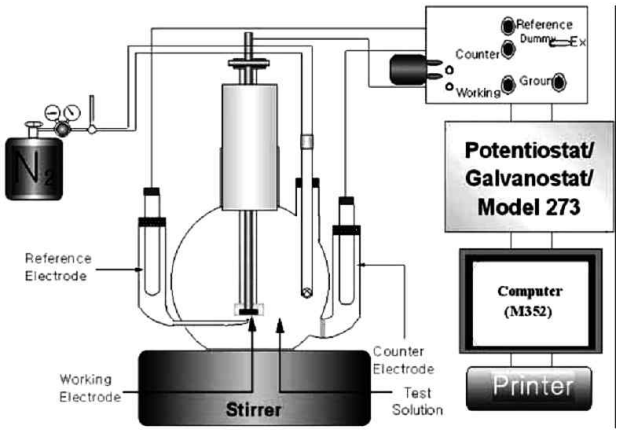


**Fig. 1 The experimental set-up for electrochemical test.**

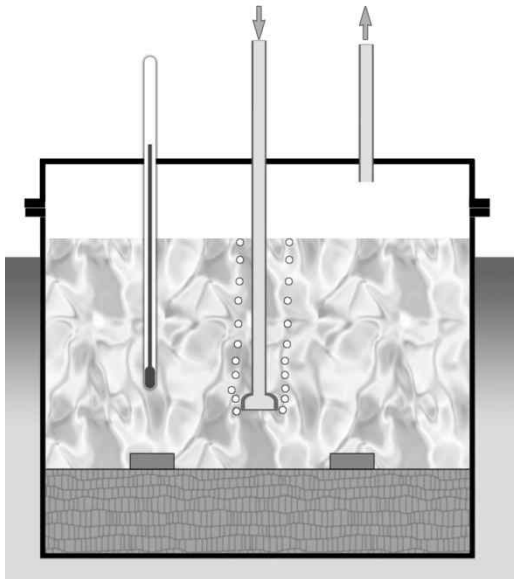

**Fig. 2 Schematic drawing of immersion test.**

- 2.0 V to - 0.8 V at the scan rate of 0.175 mV/s. All the polarization curves were conducted by Potentiostat/ Galvanostat Model 273A, EG&G.

The test set-up for immersion was shown in Fig. 2. The composition of AZ31B Mg alloy used in the immersion test is same as Table 1a. The dimension for specimens used in the immersion test is a 25 mm × 50 mm size, also were cut into a samples and polished to #800 ~ #2000 using SiC grit paper, and final polished was prepared as a mirror-like surface using a 1μm diamond paste. The electrolytes used for immersion test were same as electrochemical experiment. Also, the experiment procedures for the immersion test are as follows; under open atmosphere conditions the specimens were immersed on the glass ladder in a 1000 ml cell at room temperature during 96 hours. All specimens were ultrasonically cleaned with ethanol before and after the test, and the change of sample weight was measured before and after immersion. The surface of each sample was observed by optical microscopy (OM) and scanning electron microscopy (SEM) for identifying the types of corrosion with different electrolytes.

The corrosion rate of Mg alloy evaluated by weight loss method can be calculated as following equation (1 and 2), the corrosion rate is expressed in terms of mpy (mils/year) by calculating the mean value of the weight change of sample before and after the test [26] by several trials as following equation.

$$\text{mpy} = \frac{534W}{DAT} \tag{1}$$

$$1\text{mpy} = 0.0254\frac{mm}{yr} \tag{2}$$

## 3. Results & Discussion

Fig. 3 shows the potentiodynamic polarization curves of AZ31B Mg alloy in 0.01 M NaOH with various concentration of NaCl. First of all, There is a typical anodic polarization curve for the formation of uniform passive film in the pH12 alkaline electrolyte without chlorides after corrosion potential as reported elsewhere [11]. The polarization behavior of the AZ31B alloy in the presence of chlorides demonstrated that there are three different distinct area such as cathodic area, anodic area and pitted area while the voltage scan from cathodic area to anodic region. The corrosion potentials of the AZ31B Mg alloy for the 0.01 M NaOH, 0.01 M NaOH + 0.005 M NaCl, 0.01 M NaOH + 0.01 M NaCl and 0.01 M NaOH + 0.02 M NaCl were found to be - 1.37 V, - 1.41 V, - 1.46 V and -1.48 V respectively. Therefore, the corrosion potentials ($E_{corr}$) of the AZ31B Mg alloy were shifted to less noble direction as increasing with an increase of $Cl^-$ concentration. This behavior of corrosion potential is well agreement with increasing corrosion sensitivity of Mg alloy with increasing chloride concentration.

Also, as shown in Fig. 3, it is observed that the polarization curves of AZ31B Mg alloy in the 0.01 M NaOH + 0.005 M NaCl demonstrated two different kinds of anodic behavior: one thing is complete passive behavior and the other is pitting behavior at a higher potential region even though the experiments were conducted repeatedly at same electrolyte condition. This implies that the critical concentration of pitting for the AZ31B Mg alloy in the

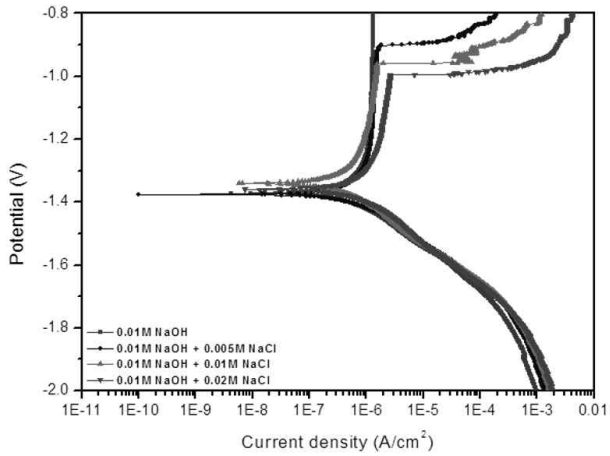


**Fig. 3 Potentiodynamic polarization curves of AZ31B Mg alloy for the 0.01 M NaOH with different NaCl concentration in aerated condition at the scan rate of 0.175 mV/s.**

0.01 M NaOH electrolyte (pH12) is below or above the concentration of 0.005 M of NaCl. Thus, the critical concentration of pitting corrosion for the Mg alloy was evaluated with 0.005 M NaCl in 0.01 M NaOH on the anodic potential at the occurrence of pitting corrosion for the chlorides concentration between the concentration of 0.005 M of NaCl and 0.01 M NaCl. Moreover, the pitting of AZ31B Mg alloy for the 0.01 M NaOH electrolyte was observed for the 0.005 M NaCl and 0.01 M NaCl concentration due to breakdown of the passive film on higher anodic potential region. The pitted region was highly localized on the surface as shown in the Fig. 3 discussed later as expected as breakdown of the film occurs at highly localized sites. Also, the pitting potential of AZ31B Mg alloy in the 0.01 M NaOH electrolyte for 0.005 M NaCl, 0.01 M NaCl and 0.02 M NaCl were measured at - 900 mV, - 960mV and - 996 mV, respectively. However, in the case of the 0.01 M NaOH electrolyte in addition to higher concentration of 0.001 M NaCl, AZ31B Mg alloy was completely passivated the entirely range of anodic polarization without breakdown of the passive film. Also, there was no observable pitting on the Mg alloy surface occurred at anodic high potential due to stable passive film formation. However, the passive current was measured with twice higher than that of chloride-free electrolyte. This implies that the passive film was unstable even though small amount of chloride ion in the electrolyte compared to chloride free electrolyte. Moreover, there was no observable pitting on the Mg alloy surface during anodic polarization curve as discussed later on surface microscopy.

It was found that the effect of electrolyte composition on the pitting for steel and stainless steel was well established by some authors [27,28] by the conventional form as a function of concentration of chloride. In other words, the effect of $[Cl^-]$ on pitting potential ($E_{pit}$) had relationship with a dependence of $E_{pit}$ on chlorine concentration. Therefore, the pitting potential as an increase of chloride concentration for the passive state metal can be expressed as the following equation ;

$$E_{pit} = A \log [Cl^-] + B \quad (3)$$

where, A and B are the constant

Previous investigator [30] was found that pitting potential for the 304 stainless steel as chloride concentration was found to be following equation;

$$E_{pit} = 0.168 - 0.88 \log [Cl^-] \quad (4)$$

The critical concentration of pitting for the system of magnesium alloy (AZ31B Mg alloy) in 0.01 M NaOH was observed 0.005 M chloride concentration as shown in Fig. 3. Moreover, it was measured that the pitting potential with an increase with chlorine concentration for the AZ31B Mg alloy with 0.01 M NaOH system.

Thus, one can derive equation (5) for $E_{pit}$ (the pitting potential) relationship as a function of chlorides by substitution to the equation (3) to the given electrochemical value on the polarization behavior of the AZ31B Mg alloy in the 0.01 M NaOH system as following equation;

$$E_{pit} = - 1.36 - 0.2 \log [Cl^-] \quad (5)$$

So, one can see that what if the pitting potential equation as a function of $[Cl^-]$ for the Mg alloy does work for the 0.02 M chloride concentration. The measured pitting potential ($E_{pit}$) for 0.02 M NaCl was - 0.996 mV compared with calculated value from the equation (5) for 1.02 V with only 0.06 V slight deviation. So, this parameter is consistent with the measured decreasing $E_{pit}$ value resulting from the calculated value based on equation (5).

The AZ31B Mg alloy with 0.01 M NaOH system was found to be very low passive current up to very high anodic potential region for the entire anodic polarization curve in the absence of chloride as proof of very stable passive film. Therefore, it can be concluded that the critical concentration of pitting for the system of magnesium alloy (AZ31B Mg alloy) in the pH12 electrolyte is about 0.005 M chloride concentration, such that small amount of chloride pollution may cause of pitting corrosion in the surface treatment.

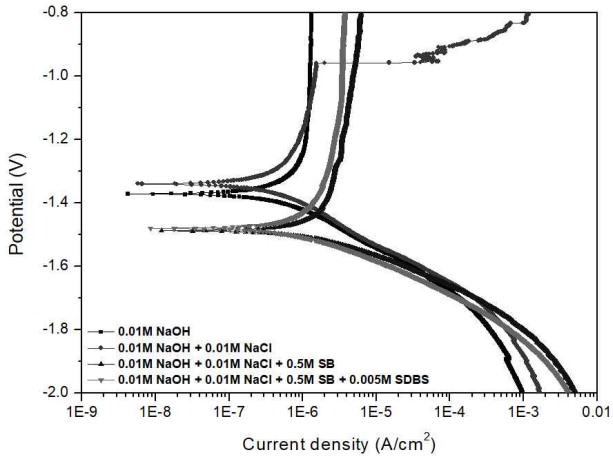


**Fig. 4 Potentiodynamic polarization curves of AZ31B Mg alloy for the 0.01 M NaOH with different NaCl concentration in aerated condition in addition with 0.5 M SB and/or 0.005 M SDBS at the scan rate of 0.175 mV/s.**

The adoption of inhibitors is one of most practical methods to preventing for metal corrosion. Especially, corrosion protection of light-weight materials such as Al alloy and Mg alloy is urgent problem due to active metals, therefore organic salt such as SB and SDBS for Al alloy [21,33] was introduced to protect corrosion in NaCl electrolyte.

Further investigation was proceeded in the presence of various inhibitors for the of Mg alloys in 0.01 M NaOH + 0.01 M NaCl solution by potentiodynamic polarization test with same scan rate. Fig. 4 showed the potentiodynamic polarization curves of AZ31B Mg alloy in 0.01 M NaOH and 0.01 M NaCl with different concentration of SB (Sodium Benzoate) and/or SDBS (Sodium Dodecylbenzene-sulphonate). The corrosion potentials of the AZ31B Mg alloy for the 0.01 M NaOH, 0.01 M NaOH + 0.01 M NaCl, 0.01 M NaOH + 0.01 M NaCl + SB and 0.01 M NaOH + 0.01 M NaCl + SB and SDBS were measured as - 1.37 V, - 1.45 V, - 1.49 V and - 1.48 V, respectively. The corrosion potential of AZ31B Mg alloy in 0.01 M NaOH (pH12) was the highest value of $E_{corr}$ (- 1.37 V) and the lowest value of $I_{corr}$ (457 nA) as shown in Fig. 4. This represents that the most stable passive film on Mg alloy surface was formed among the given 5 different electrolytes. Also, the polarization behavior of the AZ31B Mg alloy in 0.01 M NaOH with 0.01 M NaCl demonstrated that pitting corrosion occurred above pitting potential (- 0.96 V,SCE) due to breakdown of passive film on the Mg surface while the passive region was ranging from - 1.4 V to - 0.96 V.

The important parameters for the electrochemical values such as corrosion potential, corrosion current density and passive current based on Fig. 4 are summarized in Table 2. The corrosion potential for the Mg alloy in the pH12 was shifted less noble direction with 800 mV in the presence of 0.01 M chloride, however, the corrosion potential for the AZ31B Mg alloy in 0.01 M NaOH with 0.01 M NaCl in presence of inhibitor such as SB and/or SDBS was not sizable potential change for the anodic polarization curve. Nonetheless, the corrosion potentials for the Mg alloy system (pH12 with 0.01 M chloride) in the presence of inhibitor (both SB and SDBS) were shifted to less noble direction, thus inhibitors plays as an anodic inhibitor for this system.

Also, the value of passive current for the system of Mg alloy 0.01 M NaOH and Mg alloy 0.01 M NaOH + 0.01 M NaCl was measured as a value of $1.26\times10^{-6}$(A/cm$^2$) and $1.37 \times 10^{-6}$(A/cm$^2$), respectively. The passive current was not significant change in the presence of chloride which means that stable passive film formed on the Mg alloy surface although unwanted chloride ion ingression in the alkaline system

The pH12 electrolyte for Mg alloy for surface processing was used in industry. And if contaminated by chlorine ion, we can run experiment for the simulated environment as the mixture solution of 0.01 M NaOH + 0.01 M NaCl. For this result, Mg alloy in the 0.01 M NaOH + 0.01 M NaCl electrolyte appeared to form a film for typical polarization behavior in the alkaline solution at the beginning of the passive region but the passive film was destroyed after the $E_{pit}$ (- 0.96 V, $_{SCE}$). This suggests that a small amount of $Cl^-$ in the alkaline solution hinders stable film formation on passivation.

Surprisingly, polarization behavior of Mg alloy in pH12 with 0.01 M NaCl in the presence of SB and SDBS did not demonstrate the behavior of pitting corrosion for the whole anodic polarization curve. This phenomenon indicates that Mg alloy in the presence of the SB and the SDBS in the electrolyte was protected from pitting corrosion by barrier action of attacking from chlorides even at higher potential region, i.e. higher oxidizing environment. However, it is uncertain that how does inhibitors are working as strong passive film former at higher potential region on expected pitted area without inhibitors. Probably, one can be understood by XPS analysis on the Mg alloy and will be discussed later. Also, the electrochemical parameters ($E_{corr}$ and $I_{pass}$) obtained by anodic polarization behavior of Mg Alloy by adding inhibitor of 0.5 M SB and 0.5 M SB + 0.005 M SDBS in the 0.01 M NaOH + 0.01 M NaCl electrolyte were evaluated by change of electrolyte concentration. The passive current ($I_{pass}$) of Mg alloy for 0.01 M NaOH , 0.01 M NaOH + 0.01 M NaCl, 0.01 M NaOH + 0.01 M NaCl + 0.5 M SB and 0.01 M NaOH

**Table 2 Summary of the electrochemical parameters from the potentiodynamic polarization curves of AZ31B Mg alloys in the 0.01 M NaOH with different NaCl concentration in addition with SB and SDBS**

| Electrolyte composition | $E_{corr}$ (V),SCE | $I_{corr}$ (A/cm$^2$) | Passive current density(A/cm$^2$) |
|---|---|---|---|
| NaOH | -1.37 | $4.57\times10^{-7}$ | $1.26\times10^{-6}$ |
| NaOH + NaCl | -1.34 | $4.42\times10^{-7}$ | $3.07\times10^{-6}$ |
| NaOH + NaCl + SB | -1.49 | $1.69\times10^{-6}$ | $4.79\times10^{-6}$ |
| NaOH + NaCl + SB + SDBS | -1.48 | $6.14\times10^{-7}$ | $3.45\times10^{-6}$ |

**Table 3 Corrosion rate (mm/yr) of AZ31B Mg alloy by immersion test in the given electrolyte composition for 96 hr at 25 ℃**

| Electrolyte composition | Weight change(mg) | Area(cm$^2$) | mm/yr | Remarks |
|---|---|---|---|---|
| NaOH | 0.5 | 12.6 | | weight gain |
| NaOH + NaCl | - 0.5 | 11.9 | 0.0123 | |
| NaOH + NaCl + SB | - 0.4 | 9.7 | 0.0118 | |
| NaOH + NaCl + SB + SDBS | 0.2 | 9.1 | | weight gain |

+ 0.01 M NaCl + 0.5 M SB + 0.005 M SDBS was found to be $1.26\times10^{-6}$ (A/cm$^2$), $1.37\times10^{-6}$ (A/cm$^2$), $4.79\times10^{-6}$ (A/cm$^2$) and $3.45\times10^{-6}$ (A/cm$^2$), respectively as listed in Table 2. The corrosion rate in mm/yr was calculated through Faraday's law by previous investigators [30-32]. The passive current for Mg alloy in the presence of chloride before pitting is approximately same current value as that of chloride-free electrolyte. This means that thickness of passive film of Mg alloy in the absence of chlorides is almost same thickness of that of Mg alloy in the presence of chlorides.

Moreover, the passive currents for Mg alloy in the 0.01 M NaOH + 0.01 M NaCl in addition with SB and SDBS were not significantly change the passive current compared to that of Mg alloy in the 0.01 M NaOH + 0.01 M NaCl. Thus, a little change on the passive current in the presence of inhibitors probably signifies that the contribution to formation of passive film on the Mg alloy as inhibitors is less effective on the polarization curve. However, it can be proved that measurement of weight loss method in the addition of SDBS represents enhancement of the corrosion resistance of Mg alloy in the presence of chlorides as discussed later. In the presence of $Cl^-$, the passive current of Mg alloy in the electrolyte in addition with both the SB and the SDBS was not significant value compared to that of the SB only. However, corrosion resistance for both the SB and the SDBS is higher than that of the SB only by the weight loss method discussed later. Therefore, AZ31B Mg alloy have a formation of stable passive film in alkaline electrolyte (pH=12), but it was suffering from pitting corrosion with a small amount of chlorides due to breakdown of the passive film. However, new finding for the Mg alloy is that although electrolyte was contaminated by chloride ion, by adding SB and SDBS as corrosion inhibitors Mg alloy can be protected from the types of corrosion by the formation of passivation film on the surface.

Therefore, we can be concluded that the Mg alloy in pH12 with a contamination of chloride ion in the presence of inhibitors is not suffering from the pitting corrosion, but the formation of passive film is not probably as strong enough as passive film of pH12. The characteristics of passive film for Mg alloy in the 0.01 M NaOH + 0.01 M NaCl + SB and/or SDBS is similar with that of the presence of $Cl^-$. This indicates that AZ31B Mg alloys with a small amount of chloride contamination could have suffering from the pitting corrosion by the breakdown of passive film due to unstable passive film formation. However, AZ31B Mg alloys with a small amount of chloride contamination in the presence of inhibitors such as SB and SDBS could be protected from the types of corrosion by adsorption of inhibition species on the Mg alloy surface by stable film formation.

The corrosion rate of AZ31B Mg alloy by immersion test was evaluated by weight loss method in the given electrolyte composition for 96 hr at 25 ℃ as listed in Table 3. The corrosion rate evaluated by mpy(mils/yr), converted to mm/yr was calculated by changing the weight loss before and after immersion of each specimen by using the equation (1) and (2) [26] . For each immersion test,

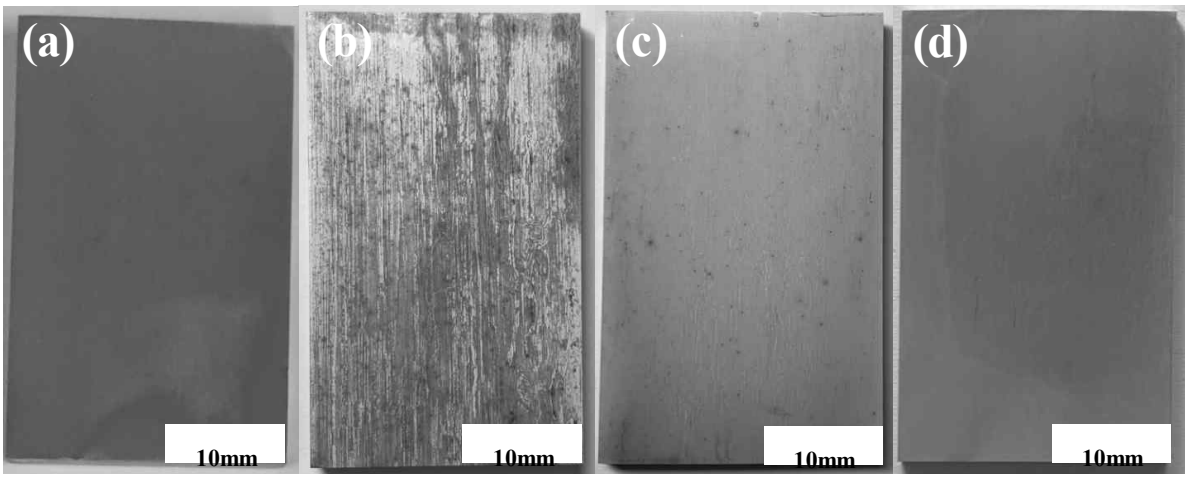


**Fig. 5 Surface observation on AZ31B Mg alloy by digital camera after immersion test for 96 hr; (a) 0.01 M NaOH, (b) 0.01 M NaOH + 0.01 M NaCl, (c) 0.01 M NaOH + 0.01 M NaCl + 0.5 M SB, (d) 0.01 M NaOH + 0.01 M NaCl + 0.5 M SB + 0.005 M SDBS.**

the 3 specimens of AZ31B alloy were immersed in each cell for the given electrolyte composition. The average weight change obtained by the 3 different specimens after immersion test was recorded by about 0.5 mg.

The corrosion rate (mm/year) of Mg alloy for 0.01 M NaOH, 0.01 M NaOH + 0.01 M NaCl, 0.01 M NaOH + 0.01 M NaCl + 0.5 M SB and 0.01 M NaOH + 0.01 M NaCl + 0.5 M SB + 0.005 M SDBS was found to be 0, 0.0123, 0.0118 and 0, respectively as listed in Table 3. The corrosion rate of Mg alloy for 0.01 M NaOH and 0.01 M NaOH + 0.01 M NaCl + 0.5 M SB + 0.005 M SDBS was measured as almost zero due to weight gain for passive film on the surface in pH12 and inhibitor deposit on the surface in addition with inhibitors. Also, this result is very consistent with the data obtained by electrochemical test on polarization behavior.

The surface microscopy of the AZ31B alloy after immersion test in a given electrolyte composition for 96 hours was recorded by digital camera (DC), optical microscope (OM) and scanning electron microscope (SEM). As shown in Fig. 5a, the surface morphology of Mg alloy in the pH12 (0.01 M NaOH) demonstrated no distinct observable change on the surface by immersion compared with surface morphology by corrosion attack as shown in Fig. 5b in the presence of chloride. This observation of no attack on the surface consistent with optical microscopy (Fig. 6a) and surface microscopy of SEM (Fig. 7a) is very well matching with the formation of strong passive film [19] on the anodic polarization. No trace of corrosion attack on the surface microscopy obtained by DC, OM and SEM is consistent with low passive current in electrochemical experiment as shown in Fig. 3. Also, polarization behavior of Mg alloy in pH12 was found to form stable passive film after corrosion potential as previous investigators [11,19]. Therefore it was confirmed that the film becomes protective and stable at higher than pH11 [13]. Fig. 5b shows the surface morphology on Mg alloy in the 0.01 M NaOH + 0.01 M NaCl after immersion test for 96 hours. There was corrosion attack on the surface with small pitting corrosion while rest area on the surface was not attacked (Fig. 5b), and pitting corrosion was randomly observed on the surface (Fig. 6b) whereas corrosion product was formed most surface. Also, Fig. 7b clearly represents the occurrence of pitting corrosion on the surface as white irregular shape of pit as shown marks of circle on the top of the corrosion pit. The pits on the Mg alloy surface with a large amount of pits were evaluated by OM. The depth of pit and width of pit were measured with 2 - 4 μm and 10 - 20 μm in the presence of chloride for 96 hours. The corrosion rate obtained by weight loss method was 0.0123 mm/yr even though corrosion rate itself is not meaningful on pitting corrosion. The surface morphology of the specimen with chloride (Fig. 5b) showed severely attacked compared with chloride free electrolyte (Fig. 5a).

The observation of pitting corrosion on the Mg alloy surface in the presence of chloride is very well in agreement with the formation of pitting corrosion on the anodic polarization curve at higher than $E_{pit}$ with abrupt increase of current in electrochemical experiment as shown in Fig. 3.

Surface morphology change in the presence of inhibitors (SB) on AZ31B Mg alloy by digital camera (Fig. 5c and d), optical microscope (Fig. 6c and d) and SEM (Fig. 7c and d) after immersion test was distinct compar-

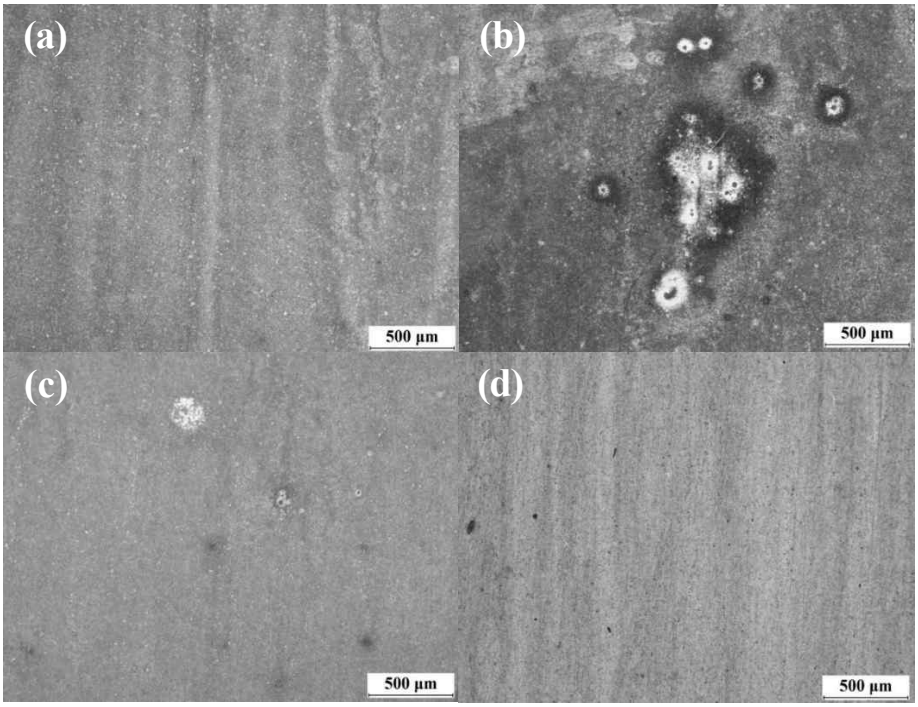


**Fig. 6 Surface microscopy of AZ31B Mg alloy by optical microscopy after immersion test for 96 hr; (a) 0.0 1 M NaOH, (b) 0.01 M NaOH + 0.01 M NaCl, (c) 0.01 M NaOH + 0.01 M NaCl + 0.5 M SB, (d) 0.01 M NaOH + 0.01 M NaCl + 0.5 M SB + 0.005 M SDBS.**

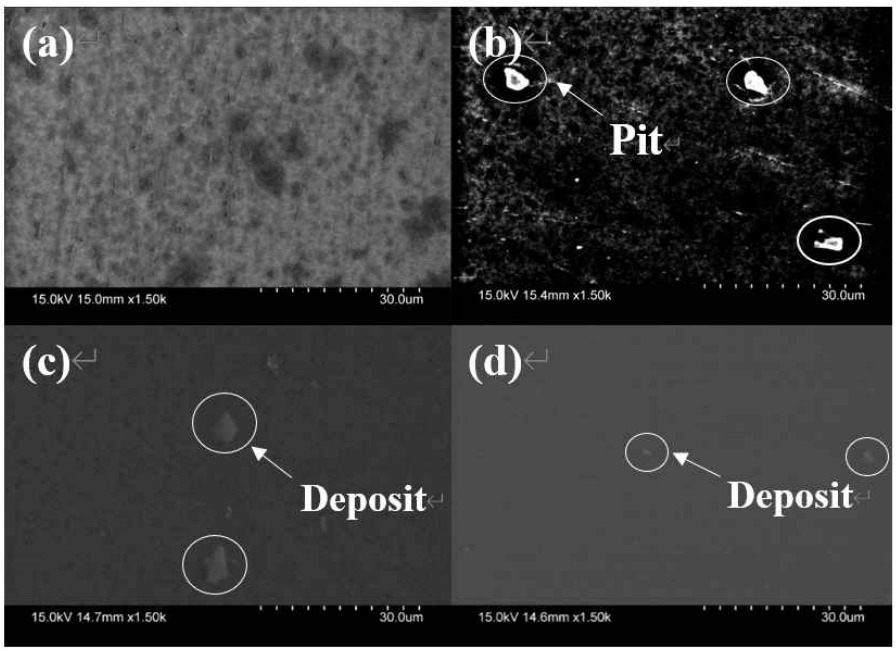


**Fig. 7 Surface microscopy of AZ31B Mg alloy by SEM after immersion test for 96 hr; 0.01 M NaOH, (b) 0.01 M NaOH + 0.01 M NaCl, (c) 0.01 M NaOH + 0.01 M NaCl + 0.5 M SB, (d) 0.01 M NaOH + 0.01 M NaCl + 0.5 M SB + 0.005 M SDBS.**

ing with corrosion surface on Mg alloy surface in the presence of chloride. M. Kaseem, M. P. Kamil *et.al* [33] was studied that effect of sodium benzoate on corrosion behavior of 6061 Al alloy was figured out stability of the film in the presence of chlorides.

By using the SB in the electrolyte, it was observed that the few of pit on surface (Fig. 6c) revealed the possibility of metastable pit on the Mg alloy surface due to instability of passive film for the SB inhibitor. With an observation by optical microscopy (Fig. 6c), the pit was a depth of 1μm and width of 30μm which was not active pits compared to observed on the active pit shown in Fig. 6b. Also, the deposit (Fig. 7c) on the Mg alloy surface as marking of circle on the top of the deposit was indicated that the film on the Mg surface was protected from the pitting corrosion as SB inhibitor. It was a few pits on the Mg surface as shown surface morphology in consistent with other observation [20] as inhibition efficiency was less effective than SDBS. Therefore, it was figured out that the adsorption of SB on the surface reduced the degree of pitting corrosion in the presence of chloride.

There is no evidence of pitting corrosion on the Mg surface as shown in Fig. 5d, 6d and Fig. 7d while both SB and SDBS were in the electrolyte as co-inhibitor. Instead, it was revealed that the occurrence of small deposit on the surface with dirt-types represents as indicative marks of circle on the top of the deposit. Therefore, the deposit on the Mg alloy surface was clearly indicated that the strong film on the Mg surface was formed by synergistic effect of two kinds of inhibitor at a same time.

Therefore, the role of inhibitors for the Mg alloy surface in the presence of chloride was explained by suppression of pitting corrosion on the anodic polarization curve at higher than $E_{pit}$ as shown in Fig. 4. It is expected result that the synergetic effect of corrosion inhibitors such as SB and SDBS could be adsorbed with a high chemical affinity at a same time on the Mg alloy surface thereby preventing the breakdown of the passive film in the presence of chloride ions.

## 4. Conclusions

In this study, the corrosion and inhibition of AZ31B alloy in the alkaline solution (pH=12) in the presence of chloride and/or with the inhibitors such as SB and SDBS was investigated by the electrochemical methods, immersion test in order to clarify chlorine ions effect on the stability of the passive film and the role of pitting corrosion at higher than $E_{pit}$ with or without inhibitors in the presence of alkaline electrolyte solution.

1) The critical concentration of pitting corrosion for Mg alloy was evaluated with 0.005 M NaCl in 0.01 M NaOH on the anodic polarization behavior.
2) The critical pitting of AZ31B Mg alloy in 0.01 M NaOH for 0.005 M NaCl, 0.01 M NaCl and 0.02 M NaCl was found to have relationship as a function of chlorides as follows;

$$E_{pit} = -1.36 - 0.2 \log [Cl^-]$$

3) When the SB only used as inhibitor, a few metastable pits were developed on the Mg surface by immersion test while no pitting corrosion on the polarization curve. Therefore, the adsorption of SB on the surface is not proper protection of pitting corrosion in the presence of chloride.
4) The role of inhibitors both SB and SDBS for the Mg alloy surface in the presence of chloride was suppressed of pitting corrosion to co-adsorb on the Mg alloy surface with a strong formation of passive film thereby preventing the initiation of the pitting corrosion.

## References


1. K. S. Choi and S. D. Choi, *J. Kor. Inst. Surf. Eng.*, p. 23944, (2011).
2. E. F. Emley, *Principle of Magnesium Technology,* pp. 30 - 31, Pergamon Press, London (1966).
3. G. L. Makar and J. Kruger, *Int. Mater. Rev.*, **38**, p. 138 (1993).
4. J. E. Gray and B. Luan, *J. Alloys Compd.*, **336**, 88 (2002).
5. W. S. Loose, *Corrosion and Protection of Magnesium, in: L. M. Pidgeon, J. C. Mathes, N. E. Woldmen (eds.)*, p. 173, ASM Int., Materials Park, OH (1946).
6. O. Lander, J. E. Lein, T. Kr Aune, and K. Nisanciogiu, *Corrosion*, **45**, 741 (1989).
7. L. Wang, T. Shinohara, and B.-P. Zhang, *Zairyo-to-Kankyo*, **58**, 105 (2009).
8. D. Thirumalaikumarasamy, K. Shanmugam, and V. Balasubramanian, *J. Magnes. Alloy.*, **2**, 36 (2014).
9. I. B. Singh, M. Singg, and S. Das, *J. Magnes. Alloy.*, **3**, 1 (2015).
10. L. Gao, C. Zhang, M. Zhang, X. Huang, and N. Sheng, *J. Alloys Compd.*, **468**, 285 (2009).
11. S. Li, A. C. Bacco, N. Birbillis, and H. Cong, *Corros. Sci.*, **112**, 596 (2016).
12. Q. Qu, J. Ma, L. Wang, L. Li, W. Bai, and Z. Ding, *Corros. Sci.*, **53**, 1186 (2011).
13. M. Pourbaix, *Atlas of Electrochemical Equilibria in Aqueous Solutions, 2nd ed.*, pp. 140 - 143, NACE, Houston (1974).
14. A. Pardo, M. C. Merino, A. E. Coy, R. Arrabal, F. Viejo, and E. Matykina, *Corros. Sci.*, **50**, 823 (2008).
15. *J. Liao, M. Hotta, and N. Yamamot*, *Corros. Sci.*, **61**, 208 (2012).
16. A. Pardo, M. C. Merino, A. E. Coy, R. Arrabal, F. Viejo, and E. Matykina, *Corros. Sci.*, **50**, 823 (2008).
17. F. Cao, G.-L. Song, and A. Atrens, *Corros. Sci.*, **111**, 835 (2016).
18. A. Sadeghi, E. Hasanpur, A. Bahmani, and K. S. Shin,

*Corros. Sci.*, **141**, 117 (2018).
19. A. Fattah-alhosseini and M. S. Joni, *J. Magnes. Aolly.*, **2**, 75 (2014).
20. L. Li, F. Pan, and J. Lei, *Magnesium Alloys - Corrosion and Surface Treatments*, p. 344, Intech, China (2011).
21. H. Gao, Q. Li, Y. Dai, F. Luo, and H. X. Zhang, *Corros. Sci.*, **52**, 1603 (2010).
22. Z. Feng, B. Hurley, J. Li, andR. Buchheit, *J. Electrochem. Soc.*, **165**, C94 (2018).
23. S. Thirugnanaselvi, S. Kuttirani, and A. R. Emelda, *T. Nonferr. Mettal. Soc.*, **24**, 1969 (2014).
24. Yu. I. Kuznetsov, A. M. Semiletov, and A. A. Chirkunov, *Int. J. Corros. Scale Inhib.*, **5**, 31 (2016).
25. F. Zucchi, V. Grassi, and F. Zanotto, *Mater. Corros.*, **60**, 199 (2009).
26. MARS G. Fontana, *Corrosion Engineering*, pp. 14 - 174, McGraw-Hill, New York (1986).
27. H. Yashiro and K. Tanno, *Corros. Sci.*, **31**, 485 (1990).
28. S. Ningshen, U. K. Mudali, and R. K. Dayal, *Br. Corros. J.*, **36**, 36 (2013).
29. J. Park, S. Matsch, and H. Böhni, *J. Electrochem. Soc.*, **149**, B34 (2002).
30. F. E. T. Heakal, A. M. Fekry, and M. A. E. B. Jibril, *Corros. Sci.*, **53**, 1174 (2011).
31. W. H. Ailor, *Handbook on corrosion testing and evaluation*, p. 174, John Wiley and Sons, New York (1971).
32. M. C. Zhao, M. Liu, and G. L. Song, *Corros. Sci.*, **50**, 3168 (2008).
33. M. Kaseem, M. P. Kamil, J. H. Kwon, and Y. G. Ko, *Surf. Coat. Technol.*, **283**, 268 (2015).